

## Reusable Heterogeneous Catalyst ( $M^{2+}$ )Al-Layered Double Hydroxide used for Oxidative Desulfurization of 4,6-Dimethyldibenzothiophene

Nur Ahmad<sup>1</sup>, Sahrul Wibiyani<sup>1</sup>, Idha Royani<sup>2</sup>, Risfidian Mohadi<sup>1,2</sup>, Aldes Lesbani<sup>1,2\*</sup>

<sup>1</sup>Research Center of Inorganic Materials and Coordination Complexes, Universitas Sriwijaya, Palembang, 30139, Indonesia

<sup>2</sup>Master of Materials Science, Graduate Program, Universitas Sriwijaya, Palembang, 30139, Indonesia

\*Corresponding author: aldeslesbani@pps.unsri.ac.id

### Abstract

Catalyst material ( $M^{2+}$ )Al-LDH was successfully prepared in this study. Characterisation analysis by XRD and FTIR. XRD analysis of Zn/Al-LDH, Mg/Al-LDH and Ni/Al-LDH showed agreement with pure LDH as seen from the JCPDS data and showed crystal forms similar to hydrotalcite, brucite and hydrotalcite respectively. FTIR analysis of the ( $M^{2+}$ )Al-LDH material showed the presence of functional groups which explain the presence of O–H stretching, O–H bending,  $CO_3^{2-}$  bonds and identified metal oxide (MO) groups from the synthesised LDH. ( $M^{2+}$ )Al-LDH has the ability to act as a catalyst for excellent desulphurisation of 4,6-dimethyldibenzothiophene with %conversion value above 90%. In addition, ( $M^{2+}$ )Al-LDH is a heterogeneous and reusable catalyst.

### Keywords

Desulfurization, Layered Double Hydroxide, Catalyst, Heterogeneity, Reuseability

Received: 21 September 2023, Accepted: 27 November 2023

<https://doi.org/10.26554/ijmr.20231315>

## 1. INTRODUCTION

The demand and need for petrochemical products, including oil, along with economic growth, results in higher demand for energy sources such as gasoline and diesel. According to predictions, demand for these fuels is expected to increase significantly, reaching around 29.6 million barrels per day by 2045 (Wang et al., 2021; Al-Samhan et al., 2022). Sulfur dioxide ( $SO_2$ ) emissions have been constantly increasing as a result of the fast expansion of heavy industrial processes (Liu et al., 2023). The combination of  $SO_2$  in the atmosphere with gaseous pollutants and particulate matter poses a significant risk to both human health and the broader atmospheric environment (Wang et al., 2019; Zhao et al., 2021).

Sulfur, present in crude oil, constitutes one of the most hazardous components. Crude oil is extensively utilized as fuel for diverse purposes. Sulfur can come from sulfides, thiophenes, and other S-containing compounds. Acid rain and harmful photochemical smog can be caused by the combustion of sulfur, which can cause damage and pollution to the ecological environment and human health (Zhu et al., 2020; Zhang et al., 2019; Tchalala et al., 2019). Sulfur serves as one of the primary contaminants within crude oil; hence, it becomes crucial to decrease its levels to adhere to standard requirements. The Environmental Protection Agency in the United States and the European Union have both developed recommendations stating that the sulfur level

of fuel should not exceed 10 parts per million (ppm) (Tripathi et al., 2019; Mahboob et al., 2022). Therefore, the petroleum industry must endeavor to remove these compounds through proper separation techniques.

Engineered separation methods such as adsorptive desulfurization, extractive desulfurization, and oxidative desulfurization are commonly used in the petroleum industry due to their ability to effectively remove sulfur from liquid fuels. These techniques are used to desulfurize sulfur compounds, thus meeting the required fuel quality standards (Malani et al., 2021). Oxidative desulfurization can convert thiophene sulfides in gasoline into thiophene sulfones that can be easily removed by the synergistic action of gasoline and catalyst. This process helps to effectively remove sulfur compounds from gasoline, providing fuel quality improves (Rajendran et al., 2022). Several catalysts have been used for oxidative desulfurization such as pentaethylenehexamine-phosphotungstic acid (Wu et al., 2023), Ni/ZnO (Zhu et al., 2023) and Polyoxometalate (Ahmad et al., 2022a).

Layered double hydroxide (LDH) has a specific surface area and is easy to produce, making it an interesting material that has attracted attention in the catalytic field due to its unique properties of layered double hydroxides (LDHs) are promising for catalytic applications Unique is unique property, including a wide range of chemicals, cost, bulk, critical surface area, excellent thermal stability and high adsorption capacity These characteristics make LDHs effective in catalytic applications Fur-

thermore, LDHs have the potential to reverse it has been well organized and redesigned, making it practical and a sustainable alternative. Their rapid and efficient manufacturing processes further enhance their appeal, providing them with many advantages in a variety of industrial applications. Where this material is expected to be effective for the desulfurization catalysis of 4,6-dimethyldibenzothiophene (Wei et al., 2020; Lozano-Lunar et al., 2023). Figure 1 illustrates the desulfurization process.

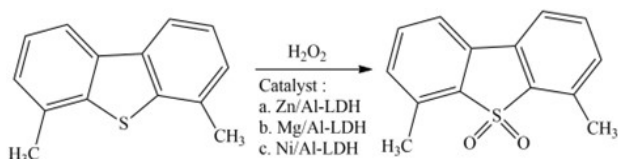


**Figure 1.** Oxidative Desulfurization of 4,6-Dimethyldibenzothiophene by Zn/Al-LDH(a), Mg/Al-LDH(b), and Ni/Al-LDH(c)

In this study, Zn/Al-LDH, Mg/Al-LDH, and Ni/Al-LDH were synthesized and used as catalysts for desulfurization of 4,6-dimethyldibenzothiophene. The sulfur-containing compound was selected as 4,6-dimethyldibenzothiophene. To ensure the success of the catalyst fabrication, XRD and FTIR measurements were carried out due to quality. It included investigation of various parameters such as time, catalyst concentration, temperature, solvent choice (n-pentane, n-hexane, and n-heptane), heterogeneous assay, and catalyst for recyclability.

## 2. EXPERIMENTAL SECTION

### 2.1 Chemical and Instrumental

Sigma-Aldrich supplied 4,6-dimethyldibenzothiophene, which was used immediately without further treatment. In addition, analytes, such as hydrogen peroxide ( $H_2O_2$ ), acetonitrile ( $CH_3CN$ ), pyridine ( $C_5H_5N$ ), zinc(II) nitrate hexahydrate ( $Zn(NO_3)_2 \cdot 6H_2O$ ), magnesium(II) nitrate hexahydrate ( $Mg(NO_3)_2 \cdot 6H_2O$ ), nickel(II) nitrate hexahydrate ( $Ni(NO_3)_2 \cdot 6H_2O$ ), n-pentane ( $C_5H_{12}$ ), n-hexane ( $C_6H_{14}$ ), n-heptane ( $C_7H_{16}$ ), aluminum nitrate nonahydrate ( $Al(NO_3)_3 \cdot 9H_2O$ ), sodium carbonate ( $Na_2CO_3$ ) and sodium hydroxide ( $NaOH$ ) were used without further purification.

Rigaku Miniflex-6000 X-ray diffractometer, EMC-18PC-UV UV-Vis spectrophotometer, Shimadzu Prestige-21 Fourier transform infrared spectrophotometer were used to analyze and analyze the qualitative and structural features of the data Primary objectives quality and composition, good sense and that was it.

### 2.2 Preparation of ( $M^{2+}$ )Al-Layered Double Hydroxide

Zinc(II), magnesium(II), and nickel(II) nitrate hexahydrate, each at a concentration of 0.75 M, and 0.25 M aluminum, are dissolved in 100 mL of distilled water to create the ( $M^{2+}$ )Al-layered double hydroxide nitrate synthesis. The resulting solution was stirred for 2 h. A 2:1 mixture of  $NaOH$  and  $Na_2CO_3$  was slowly added to the solution until its pH reached 10. The mixture was stirred again at  $70^\circ C$  for 17 h after which the mixture was filtered, and the resulting product was given dried to give two ( $M^{2+}$ )Al-layered hydroxides (Mohadi et al., 2023). The Mariel

synthesis was determined using a Rigaku Miniflex-6000 X-ray diffractometer and a Shimadzu Prestige-21 Fourier transform infrared spectrometer.

### 2.3 Oxidative Desulfurization Method

The catalytic oxidative desulfurization reaction was carried out in a 100 mL bifurcated flask under magnetic stirring at 300 rpm, then a solution containing 500 ppm 4,6-dimethyldibenzothiophene as initial concentration was added to the flask and a thickener in 30 mL of n-hexane which was formed by absorption, a it acted as solvent and then 0.25 g of ( $M^{2+}$ )Al-Layered double hydroxide was added to the flask as catalyst. To start the reaction, 1 mL of hydrogen peroxide was added as a catalyst, and 3 mL of acetonitrile was added as an eluent. The temperature of the reaction is  $323K$  (Ahmad et al., 2022b). The sulfur conversion of dibenzothiophene was analyzed using Equation 1.

$$\% \text{Sulphur Conversion} = \frac{C_0 - C_f}{C_0} \times 100\% \quad (1)$$

The symbols  $C_0$  and  $C_f$  represent the initial and final concentrations of 4,6-dimethyldibenzothiophene, respectively.

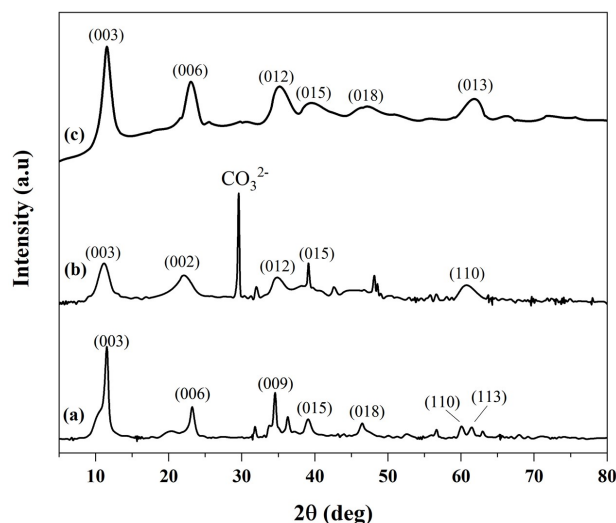
### 2.4 Heterogeneity Test

For the heterogeneity test, 500 ppm of 4,6-dimethyldibenzothiophene was desulfurized in 30 mL of n-hexane at  $323 K$  for 10 min. After the initial desulfurization, the catalyst and the 4,6-dimethyldibenzothiophene solution were separated. The separated 4,6-dimethyldibenzothiophene solution was then subjected to another desulfurization process, which lasted for 20-30 min at  $323 K$ . The main objective was to determine the sulfur conversion of 4,6-dimethyldibenzothiophene after the second and subsequent desulfurization steps (Ahmad et al., 2023).

## 3. RESULTS AND DISCUSSION

X-ray diffraction (XRD) analysis was employed to investigate the crystal structure of Zn/Al-LDH, Mg/Al-LDH and Ni/Al-LDH. The XRD pattern of the synthesized material demonstrated a close match with the characteristic pattern of pure LDH, as depicted in Figure 2. In Figure 2(a), the X-ray diffraction (XRD) analysis of Zn/Al LDH reveals clear and distinct diffraction peaks observed at specific  $2\theta$  values  $11.31^\circ$ ,  $23.10^\circ$ ,  $34.59^\circ$ ,  $39.26^\circ$ ,  $46.40^\circ$ ,  $59.77^\circ$ , and  $61.38^\circ$ . These peaks can be attributed to the crystal planes (003), (006), (009), (015), (018), (110), and (113) of the hydrotalcite-like LDH (JCPDS no. 38-0486). The presence of such well-defined peaks strongly suggests the presence of crystal structures in the Zn/Al-LDH sample (Mallakpour et al., 2023). Based on data from the Joint Committee on Powder Reaction Standards (JCPDS) File No. 20-0658 corresponds to the synthesized Mg/Al-LDH material (Juleanti et al., 2021). The presence of peaks at  $2\theta$  values on Mg/Al-LDH Figure 2(b) of  $11.31^\circ$  in the XRD pattern indicates the space or distance between two adjacent metal hydroxide sheets in the synthesized Mg/Al-LDH,  $22.22^\circ$ ,  $34.88^\circ$ ,  $39.11^\circ$ , and  $60.9^\circ$ , corresponding to the (003), (002), (012), (015), and (110) diffraction planes of the layered structure and MgAl/LDH with a

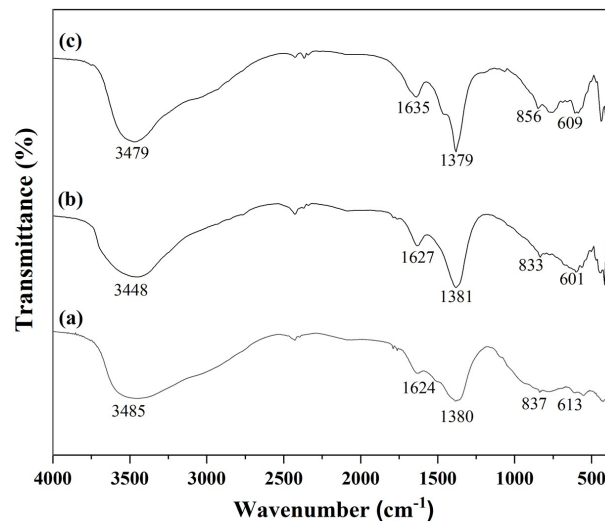
brucite-like crystal structure, confirmed the successful synthesis of Mg/Al-LDH powder (Tran et al., 2018; Huang et al., 2023). The X-ray diffraction (XRD) pattern of the Ni/Al-LDH material is presented in Figure 2(c). The pattern exhibits prominent  $2\theta$  diffraction peaks observed at  $11.60^\circ$ ,  $22.96^\circ$ ,  $35.17^\circ$ , and  $39.26^\circ$ , which can be assigned to the reflections of (003), (006), (012), and (015), respectively. These reflections correspond to the natural form of a hydrotalcite-like structure, as indicated by the JCPDS file number 33-0429 (Machrouhi et al., 2023).



**Figure 2.** X-Ray Diffraction of Zn/Al-LDH (a), Mg/Al-LDH (b), and Ni/Al-LDH (c)

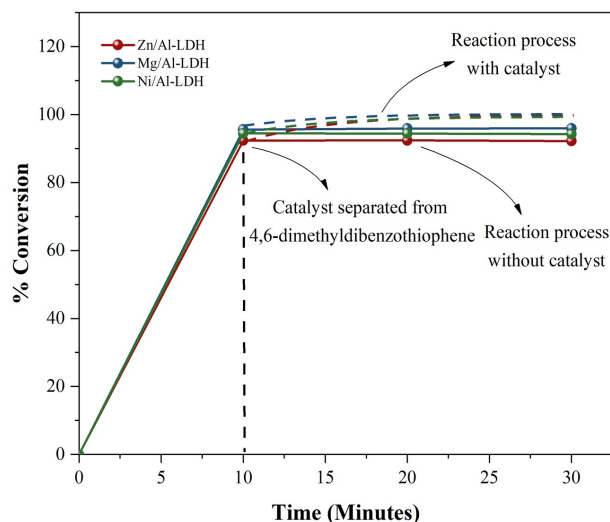
Figure 3 displays the wave number peaks of Zn/Al-LDH in Figure 3(a), Mg/Al-LDH in Figure 3(b), and Ni/Al-LDH in Figure 3(c) to analyze the functional groups present in these materials. Notably, all three materials exhibit peaks at approximately  $3450\text{ cm}^{-1}$ , which are attributed to the OH stretching vibrations of water molecules bound to the interlayer of  $\text{CO}_3^{2-}$ . Additionally, there are peaks around  $1380\text{ cm}^{-1}$ , indicating the presence of  $\text{CO}_3^{2-}$  ions in the structures of these materials (Qin et al., 2023; Lv et al., 2022; Priatna et al., 2023). Spectral analysis of the materials showed characteristic peaks in all three materials, such as O–H bending at a wave number around  $1630\text{ cm}^{-1}$  and metal oxygen bonds (M–O) at wave numbers around  $600\text{ cm}^{-1}$  and  $830\text{ cm}^{-1}$ , indicating the presence of specific functional groups and metal-oxygen bonds in the samples such as Zn–O, Mg–O, Ni–O, and Al–O (Yuliasari et al., 2022; Intachai et al., 2021; Mahjoubi et al., 2017).

The heterogeneity test is used to find out whether the catalyst used is homogeneous or heterogeneous. Homogeneous catalysts dissolve in reactants or reaction products, Heterogeneous catalysts have the advantage of being insoluble in reactants so that they can be separated (Houda et al., 2018). In this study, the heterogeneity test was conducted at  $323\text{ K}$  for 10 minutes. After the test, the catalyst and 4,6-dimethyldibenzothiophene solution were separated. The reaction process was then allowed to continue for 20-30 minutes in the absence of the catalyst. Seen



**Figure 3.** FTIR Spectrum of Zn/Al-LDH (a), Mg/Al-LDH (b), and Ni/Al-LDH (c)

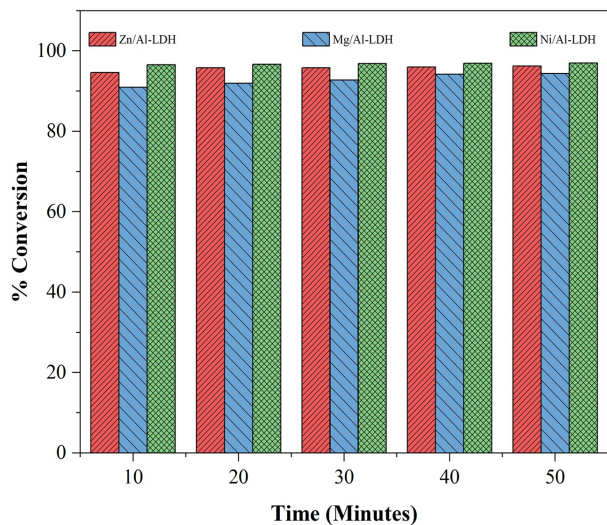
in Figure 4. at the  $10^{\text{th}}$  minute after the catalyst was separated from 4,6-dimethyldienzo thiophene the reaction was linear, the %conversion no longer increased, this indicates that the catalyst used was heterogeneous. The catalyst can be reused after separation, improving cost efficiency and environmental sustainability. Processes such as heat treatment, distillation, or surface regeneration can be adopted, restoring their catalytic properties and extending their lifetime Catalytic properties is uniquely disassembled and recycled for easy efficiency and cost-effectiveness in its industrial applications (Pei et al., 2023; Polikarpova et al., 2020).



**Figure 4.** Heterogeneity Test of Catalyst Zn/Al-LDH (a), Mg/Al-LDH (b), and Ni/Al-LDH (c)

Figure 5 illustrates the optimal desulfurization time for Zn/Al-LDH, Mg/Al-LDH, and Ni/Al-LDH in the treatment of 4,6-dime-

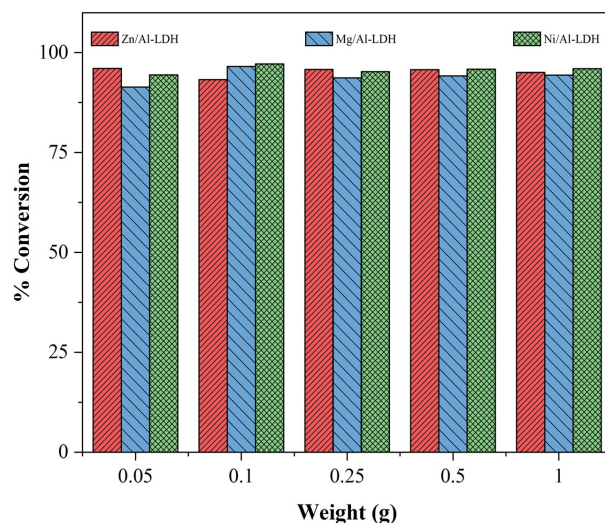
thyldibenzothiophene. The most favorable time for all three materials was found to be at the 40<sup>th</sup> minute. At this point, the sulfur conversion rates were measured at 95.99%, 94.15%, and 96.92% for Zn/Al-LDH, Mg/Al-LDH, and Ni/Al-LDH, respectively. As the reaction time increases, the percentage of conversion also rises, reaching a linear trend under the optimal conditions. Thus, the desulfurization time factor plays a crucial role (Lin et al., 2020; Zhou et al., 2021). The order of the highest to lowest conversion rates observed at the optimum conditions is Ni/Al-LDH>Zn/Al-LDH>Mg/Al-LDH.



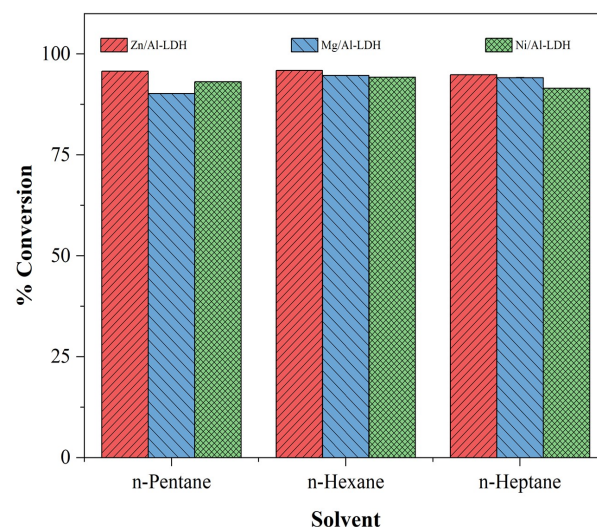
**Figure 5.** Oxidative Desulfurization of 4,6-dimethyldibenzothiophene by Catalyst Zn/Al-LDH (a), Mg/Al-LDH (b), and Ni/Al-LDH (c) on Reaction Time Effect

Figure 6 illustrates the most effective catalyst dose for desulfurizing 4,6-dimethyldibenzothiophene using the Zn/Al-LDH catalyst was found to be 0.05 g, resulting in a %conversion value of 96.04%. On the other hand, for the Mg/Al-LDH and Ni/Al-LDH catalysts, the optimal catalyst dose was 0.1 g, leading to %conversion values of 96.55% and 97.14%, respectively. In the absence of a catalyst, the rate of sulfur dissociation is negligible. By adding a catalyst and gradually increasing its concentration, the sulfur removal rate increases, eventually reaching an optimum level. However, when the catalyst concentration exceeds this optimum point, the efficiency begins to decrease. This decrease occurs because an excessive amount of catalyst saturates the system, resulting in increased sulfuration. At this point, the catalyst is fully excited, no longer facilitating the desulfurization reactions. Specifically, there is a critical point where the efficiency of the catalyst is high, beyond this point results in decreasing returns due to surface saturation (Chang et al., 2021; Subhan et al., 2019).

Figure 7 illustrates the impact of different solvents on the oxidative desulfurization of 4,6-dimethyldibenzothiophene. Among the solvents tested, n-hexane demonstrated superior effectiveness compared to n-pentane and n-heptane, as evidenced by the %conversion values obtained. When n-hexane was employed as the solvent, the %conversion values for Zn/Al-LDH, Mg/Al-LDH,



**Figure 6.** Oxidative Desulfurization of 4,6-dimethyldibenzothiophene by Catalyst Zn/Al-LDH (a), Mg/Al-LDH (b), and Ni/Al-LDH (c) on Catalyst Dosage Effect



**Figure 7.** Oxidative Desulfurization of 4,6-dimethyldibenzothiophene by Catalyst Zn/Al-LDH (a), Mg/Al-LDH (b), and Ni/Al-LDH (c) on Solvent Effect

and Ni/Al-LDH were measured at 95.89%, 94.65%, and 94.23%, respectively. The superiority of n-hexane can be attributed to its low polarity and inertness towards 4,6-dimethyldibenzothiophene. These characteristics enable an efficient extraction or separation process during oxidative desulfurization. As a result, n-hexane is deemed more suitable for this particular desulfurization reaction due to its favorable properties, which enhance the overall efficiency of the process (Zhuang et al., 2018). n-heptane exhibits a slightly higher boiling point and polarity compared to n-hexane. These differences could potentially result in varying extraction efficiencies and reaction kinetics. Although both

n-pentane and n-heptane can be used in the desulfurization process of 4,6-dimethyldibenzothiophene, n-hexane proved to be a more appropriate choice due to its ideal combination of low polarity, favorable solvent properties, and compatibility with sulfur compounds (Privat et al., 2009).

The most favorable temperature for desulfurization of 4,6-dimethyldibenzothiophene using different LDH catalysts was determined as Zn/Al-LDH catalyst exhibited optimal performance at 30°C, achieving a conversion rate of 95.77%. For the Mg/Al-LDH catalyst, the ideal temperature was found to be 50°C, leading to a conversion rate of 94.65%. Lastly, the Ni/Al-LDH catalyst demonstrated its best performance at 40°C, with a conversion rate of 95.29%. The temperature effect on the desulfurization process is visually depicted in Figure 8. The experiment covered a temperature range from 30°C to 50°C for the oxidative desulfurization process. Notably, higher temperatures were observed to enhance molecular diffusion rates and promote increased interactions between 4,6-dimethyldibenzothiophene and the catalyst, resulting in a more efficient desulfurization process (Cao et al., 2020).

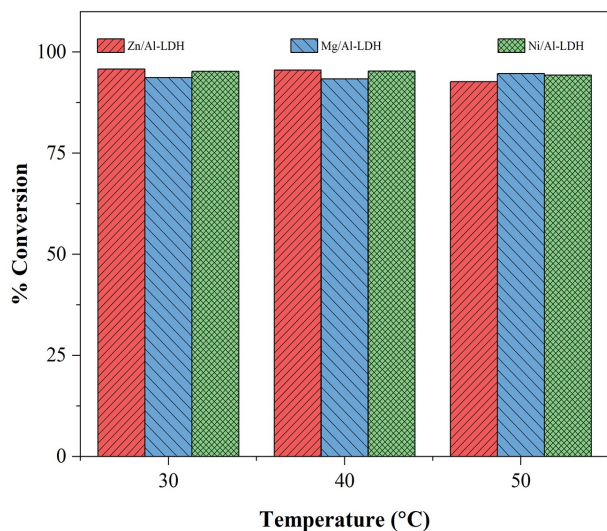


**Figure 8.** Oxidative Desulfurization of 4,6-dimethyldibenzothiophene by Catalyst Zn/Al-LDH (a), Mg/Al-LDH (b), and Ni/Al-LDH (c) on Temperature Effect

Zn/Al-LDH, Mg/Al-LDH, and Ni/Al-LDH catalysts underwent a regeneration test to evaluate their reusability for the desulfurization of 4,6-dimethyldibenzothiophene. In this test, the catalyst used in the desulfurization process was separated from 4,6-dimethyldibenzothiophene and repeatedly reused to assess its efficiency. The results, depicted in Figure 9, showed that these catalysts could be reused up to three times with %conversion values remaining effective. Although there was a slight decrease in %conversion values, they still remained within the range of 90% and above. For industrial applications, the ability to achieve rapid separation and efficient recycling of catalysts after catalytic reactions is crucial. This helps in reducing production costs and reducing waste. Efficient catalyst separation

increases system efficiency and cost. Additionally, the efficient use of recycling materials reduces the environmental impact associated with process waste, ensures more efficient use of available resources therefore power generation rapid separation and recycling of catalysts plays an important role in increasing efficiency, cost effectiveness and sustainability in the industrial sector (Miceli et al., 2021).

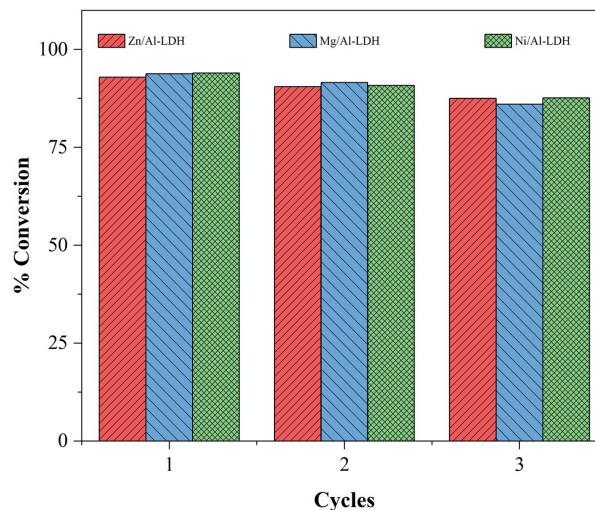


**Figure 9.** Reusability of catalyst Zn/Al-LDH (a), Mg/Al-LDH (b), and Ni/Al-LDH (c) on oxidative desulfurization of 4,6-dimethyldibenzothiophene

#### 4. CONCLUSION

The research has successfully synthesized ( $M^{2+}$ )Al-Layered Double Hydroxide, as evidenced by the results obtained from XRD and FTIR characterization analyses, which support the achievement of synthesis in this study. The ( $M^{2+}$ )Al-Layered Double Hydroxide material acts as a heterogeneous catalyst that can be separated from 4,6-dimethyldibenzothiophene and reused for desulfurization purposes. Due to its heterogeneous nature, the material demonstrates reusability, and even after three uses, its effectiveness in desulfurizing 4,6-dimethyldibenzothiophene remains high, with %conversion values consistently at 87% and above. The study revealed that the optimal desulfurization time for all three catalysts was at the 40<sup>th</sup> minute. Furthermore, the optimum dosage for ZnAl/LDH catalyst was 0.05 g, while for Mg/Al-LDH and Ni/Al-LDH, it was 0.1 g. The optimal temperatures for Zn/Al-LDH, Mg/Al-LDH, and Ni/Al-LDH were found to be 30°C, 50°C, and 40°C, respectively. Additionally, n-hexane emerged as the more suitable solvent for the desulfurization process. These findings highlight the potential of ( $M^{2+}$ )Al-Layered Double Hydroxide as an effective catalyst for desulfurization applications.

## 5. ACKNOWLEDGEMENT

The research was supported by the Hibah Profesi Universitas Sriwijaya 2023 (Grand Number SP DIPA-023.17.2.677515/2023, SK Rektor 0187/UN9.3.1/SK/2023) as an additional output. The authors would like to acknowledge the Research Center of Inorganic Materials at Sriwijaya University for providing access to their instruments, which facilitated the progress of this study.

## REFERENCES

- Ahmad, N., M. Badaruddin, N. Yuliasari, F. S. Arsyad, and A. Lesbani (2022a). Highly Efficient Catalytic Oxidative Desulfurization of Dibenzothiophene using Layered Double Hydroxide Modified Polyoxometalate Catalyst. *Bulletin of Chemical Reaction Engineering & Catalysis*, **17**(4); 821–830
- Ahmad, N., A. Wijaya, E. S. Fitri, F. S. Arsyad, R. Mohadi, and A. Lesbani (2022b). Catalytic Oxidative Desulfurization of Dibenzothiophene by Composites Based Ni/Al-Oxide. *Science and Technology Indonesia*, **7**(3); 385–391
- Ahmad, N., N. Yuliasari, F. S. Arsyad, I. Royani, R. Mohadi, and A. Lesbani (2023). Catalytic Oxidative Desulfurization of Dibenzothiophene by Heterogeneous  $M^{2+}$ /Al-Layered Double Hydroxide ( $M^{2+} = Zn, Mg, Ni$ ) Modified Zinc Oxide. *Iranian Journal of Catalysis*, **13**(1); 35–45
- Al-Samhan, M., J. Al-Fadhli, A. M. Al-Otaibi, F. Al-Attar, R. Bouresli, and M. S. Rana (2022). Prospects of Refinery Switching from Conventional to Integrated: An Opportunity for Sustainable Investment in the Petrochemical Industry. *Fuel*, **310**; 122161
- Cao, Y., H. Wang, R. Ding, L. Wang, Z. Liu, and B. Lv (2020). Highly Efficient Oxidative Desulfurization of Dibenzothiophene Using Ni Modified  $MoO_3$  Catalyst. *Applied Catalysis A: General*, **589**; 117308
- Chang, H., H. Yi, and J. Zhang (2021). Preparation of a NiO– $Bi_2WO_6$  Catalyst and Its Photocatalytic Oxidative Desulfurization Performance. *Colloid and Interface Science Communications*, **41**; 100381
- Houda, S., C. Lancelot, P. Blanchard, L. Poinel, and C. Lamonier (2018). Oxidative Desulfurization of Heavy Oils with High Sulfur Content: A Review. *Catalysts*, **8**(9); 344
- Huang, Y., X. Fan, H. Wang, Z. Li, D. Xiong, and Y. Pei (2023). Tuning Mg-Al Layered Double Hydroxides Synthesized from the Novel Ionic Liquid-Based Surfactant-Free Microemulsion for Efficiently Phosphate Removal in Aqueous Solutions. *Journal of Molecular Liquids*, **382**; 121826
- Intachai, S., T. Nakato, and N. Khaorapong (2021). ZnO Decorated on Low Carbonate NiAl-Layered Double Hydroxide As Efficient Photocatalyst for Methyl Orange Degradation. *Applied Clay Science*, **201**; 105927
- Juleanti, N., N. R. Palapa, T. Taher, N. Hidayati, B. I. Putri, and A. Lesbani (2021). The Capability of Biochar-Based CaAl and MgAl Composite Materials As Adsorbent for Removal Cr(VI) in Aqueous Solution. *Science and Technology Indonesia*, **6**(3); 196–203
- Lin, Y., L. Feng, X. Li, Y. Chen, G. Yin, and W. Zhou (2020). Study on Ultrasound-Assisted Oxidative Desulfurization for Crude Oil. *Ultrasonics Sonochemistry*, **63**; 104946
- Liu, P., S. Yang, J. Hu, and H. Wang (2023). Numerical Analysis of  $SO_2$  Removal Characteristics in Industrial Flue Gas Desulfurization Reactor by Spray Drying Adsorption. *Separation and Purification Technology*, **323**; 124475
- Lozano-Lunar, A., R. Otero, J. I. Álvarez, J. R. Jiménez, and J. M. Fernández-Rodríguez (2023). Application of Layer Double Hydroxide in Cementitious Matrices for the Improvement of the Double Barrier Technique in the Immobilisation of Lead Waste. *Applied Clay Science*, **238**; 106938
- Lv, H., H. Rao, Z. Liu, Z. Zhou, Y. Zhao, H. Wei, and Z. Chen (2022). NiAl Layered Double Hydroxides with Enhanced Inter-layer Spacing Via Ion-Exchange As Ultra-High Performance Supercapacitors Electrode Materials. *Journal of Energy Storage*, **52**; 104940
- Machrouhi, A., M. Khnifira, W. Boumya, M. Sadiq, M. Abdennouri, A. Elhalil, F. Mahjoubi, and N. Barka (2023). Experimental and Density Functional Theory Studies of Methyl Orange Adsorption on Ni-Al/LDH Intercalated Sodium Dodecyl Sulfate. *Chemical Physics Impact*, **6**; 100214
- Mahboob, I., I. Shafiq, S. Shafique, P. Akhter, M. Hussain, and Y. K. Park (2022). Effect of Active Species Scavengers in Photocatalytic Desulfurization of Hydrocracker Diesel Using Mesoporous  $Ag_3VO_4$ . *Chemical Engineering Journal*, **441**; 136063
- Mahjoubi, F. Z., A. Khalidi, M. Abdennouri, and N. Barka (2017). Zn–Al Layered Double Hydroxides Intercalated with Carbonate, Nitrate, Chloride and Sulphate Ions: Synthesis, Characterisation and Dye Removal Properties. *Journal of Taibah University for Science*, **11**(1); 90–100
- Malani, R. S., A. H. Batghare, J. B. Bhasarkar, and V. S. Moholkar (2021). Kinetic Modelling and Process Engineering Aspects of Biodesulfurization of Liquid Fuels: Review and Analysis. *Bioresource Technology Reports*, **14**; 100668
- Mallakpour, S., E. Azadi, and M. Dinari (2023). Removal of Cationic and Anionic Dyes Using Ca-Alginate and Zn-Al Layered Double Hydroxide/metal-Organic Framework. *Carbohydrate Polymers*, **301**; 120362
- Miceli, M., P. Frontera, A. Macario, and A. Malara (2021). Recovery/reuse of Heterogeneous Supported Spent Catalysts. *Catalysts*, **11**(5); 591
- Mohadi, R., N. R. Palapa, S. Wibiyana, Mardiyanto, Rohmatullaili, E. S. Fitri, and A. Lesbani (2023). Catalytic Oxidative Desulfurization of 4-Methyldibenzothiophene by Ni/Al Modified Titanium Dioxide and Zinc Oxide. *Science and Technology Indonesia*, **8**(3); 414–421
- Pei, T., Y. Chen, H. Wang, and L. Xia (2023). Heteropolyacid Ionic Liquid-Based MCF: An Efficient Heterogeneous Catalyst for Oxidative Desulfurization of Fuel. *Materials*, **16**(8); 3195
- Polikarpova, P., A. Akopyan, A. Shlenova, and A. Anisimov (2020). New Mesoporous Catalysts with Brønsted Acid Sites for Deep Oxidative Desulfurization of Model Fuels. *Catalysis Communications*, **146**; 106123
- Priatna, S., Y. Hakim, S. Wibyan, S. Sailah, and R. Mohadi (2023). Interlayer Modification of West Java Natural Bentonite as Haz-

- ardous Dye Rhodamine B Adsorption. *Science and Technology Indonesia*, **8**(2); 160–169
- Privat, R., F. Garcia, J.-N. I. Jaubert, and M. Moliere (2009). Ethanol-Hydrocarbon Blend Vapor Prediction. In *Turbo Expo: Power for Land, Sea, and Air*, volume 48821. pages 377–387
- Qin, J., H. Shi, Q. Lv, M. He, Y. Xu, M. Chen, X. Chen, J. Zhang, Y. Liu, and J. Yu (2023). Enhanced Adsorption Effect of Defect Ordering Mg/Al on Layered Double Hydroxides Nanosheets with Highly Efficient Removal of Congo Red. *Materials & Design*, **232**; 112084
- Rajendran, A., H. X. Fan, T. Y. Cui, J. Feng, and W. Y. Li (2022). Octamolybdates Containing MoV and MoVI Sites Supported on Mesoporous Tin Oxide for Oxidative Desulfurization of Liquid Fuels. *Journal of Cleaner Production*, **334**; 130199
- Subhan, S., A. U. Rahman, M. Yaseen, H. U. Rashid, M. Ishaq, M. Sahibzada, and Z. Tong (2019). Ultra-Fast and Highly Efficient Catalytic Oxidative Desulfurization of Dibenzothiophene at Ambient Temperature Over Low Mn Loaded Co-Mo/Al<sub>2</sub>O<sub>3</sub> and Ni-Mo/Al<sub>2</sub>O<sub>3</sub> Catalysts Using NaClO As Oxidant. *Fuel*, **237**; 793–805
- Tchalala, M., P. Bhatt, K. Chappanda, S. Tavares, K. Adil, Y. Belmabkhout, A. Shkurenko, A. Cadiau, N. Heymans, G. De Weireld, et al. (2019). Fluorinated MOF Platform for Selective Removal and Sensing of SO<sub>2</sub> from Flue Gas and Air. *Nature Communications*, **10**(1); 1328
- Tran, H. N., C. C. Lin, and H. P. Chao (2018). Amino Acids-Intercalated Mg/Al Layered Double Hydroxides As Dual-Electronic Adsorbent for Effective Removal of Cationic and Oxyanionic Metal Ions. *Separation and Purification Technology*, **192**; 36–45
- Tripathi, N., R. S. Singh, and C. D. Hills (2019). Microbial Removal of Sulphur from Petroleum Coke (Petcoke). *Fuel*, **235**; 1501–1505
- Wang, H., B. Yuan, R. Hao, Y. Zhao, and X. Wang (2019). A Critical Review on the Method of Simultaneous Removal of Multi-Air-Pollutant in Flue Gas. *Chemical Engineering Journal*, **378**; 122155
- Wang, L., F. Ma, T. Niu, and C. Liang (2021). The Importance of Extreme Shock: Examining the Effect of Investor Sentiment on the Crude Oil Futures Market. *Energy Economics*, **99**; 105319
- Wei, X., D. Zheng, M. Zhao, H. Chen, X. Fan, B. Gao, L. Gu, Y. Guo, J. Qin, and J. Wei (2020). Cross-Linked Polyphosphazene Hollow Nanosphere-Derived N/P-Doped Porous Carbon with Single Nonprecious Metal Atoms for the Oxygen Reduction Reaction. *Angewandte Chemie*, **132**(34); 14747–14754
- Wu, C., C. Chen, Z. Qi, J. Chen, Q. Wang, C. Ye, and T. Qiu (2023). Facile Synthesis of Efficient Pentaethylenhexamine-Phosphotungstic Acid Heterogeneous Catalysts for Oxidative Desulfurization. *Chinese Journal of Chemical Engineering*, **63**; 140–147
- Yuliasari, N., A. F. Badri, A. Wijaya, P. M. S. B. N. Siregar, R. Mohadi, and A. Lesbani (2022). Modification of Mg/Al-LDH Intercalated Metal Oxide (Mg/Al-Ni) to Improve the Performance of Methyl Orange and Methyl Red Dyes Adsorption Process. *Science and Technology Indonesia*, **7**(3); 275–283
- Zhang, Y., Z. Chen, X. Liu, Z. Dong, P. Zhang, J. Wang, Q. Deng, Z. Zeng, S. Zhang, and S. Deng (2019). Efficient SO<sub>2</sub> Removal Using a Microporous Metal–Organic Framework with Molecular Sieving Effect. *Industrial & Engineering Chemistry Research*, **59**(2); 874–882
- Zhao, Z., Y. Zhang, W. Gao, J. Baleta, C. Liu, W. Li, W. Weng, H. Dai, C. Zheng, and X. Gao (2021). Simulation of SO<sub>2</sub> Absorption and Performance Enhancement of Wet Flue Gas Desulfurization System. *Process Safety and Environmental Protection*, **150**; 453–463
- Zhou, X., X. Pei, R. Wang, and T. Zhao (2021). Catalytic Conversion for Hydrogen Sulfide. *Aerosol and Air Quality Research*, **21**(9); 210065
- Zhu, H., W. Lin, Q. Li, Y. Hu, S. Guo, C. Wang, and F. Yan (2020). Bipyridinium-Based Ionic Covalent Triazine Frameworks for CO<sub>2</sub>, SO<sub>2</sub>, and NO Capture. *ACS Applied Materials & Interfaces*, **12**(7); 8614–8621
- Zhu, H. Y., N. Y. Shi, D. Y. Liu, R. Li, J. G. Yu, Q. T. Ma, T. Y. Li, H. Ren, Y. Pan, and Y. Q. Liu (2023). New Insights into the Mechanism of Reactive Adsorption Desulfurization on Ni/ZnO Catalysts: Theoretical Evidence Showing the Existence of Interfacial Sulfur Transfer Pathway and the Essential Role of Hydrogen. *Petroleum Science*, **20**(5); 3240–3250
- Zhuang, X., Z. Zhang, Y. Wang, and Y. Li (2018). The Effect of Alternative Solvents to N-Hexane on the Green Extraction of Litsea Cubeba Kernel Oils As New Oil Sources. *Industrial Crops and Products*, **126**; 340–346